

NASA/TM—2010-216918



A Heat Transfer Investigation of Liquid and Two-Phase Methane

Jonathan Van Noord
Glenn Research Center, Cleveland, Ohio

November 2010

NASA STI Program . . . in Profile

Since its founding, NASA has been dedicated to the advancement of aeronautics and space science. The NASA Scientific and Technical Information (STI) program plays a key part in helping NASA maintain this important role.

The NASA STI Program operates under the auspices of the Agency Chief Information Officer. It collects, organizes, provides for archiving, and disseminates NASA's STI. The NASA STI program provides access to the NASA Aeronautics and Space Database and its public interface, the NASA Technical Reports Server, thus providing one of the largest collections of aeronautical and space science STI in the world. Results are published in both non-NASA channels and by NASA in the NASA STI Report Series, which includes the following report types:

- **TECHNICAL PUBLICATION.** Reports of completed research or a major significant phase of research that present the results of NASA programs and include extensive data or theoretical analysis. Includes compilations of significant scientific and technical data and information deemed to be of continuing reference value. NASA counterpart of peer-reviewed formal professional papers but has less stringent limitations on manuscript length and extent of graphic presentations.
- **TECHNICAL MEMORANDUM.** Scientific and technical findings that are preliminary or of specialized interest, e.g., quick release reports, working papers, and bibliographies that contain minimal annotation. Does not contain extensive analysis.
- **CONTRACTOR REPORT.** Scientific and technical findings by NASA-sponsored contractors and grantees.

- **CONFERENCE PUBLICATION.** Collected papers from scientific and technical conferences, symposia, seminars, or other meetings sponsored or cosponsored by NASA.
- **SPECIAL PUBLICATION.** Scientific, technical, or historical information from NASA programs, projects, and missions, often concerned with subjects having substantial public interest.
- **TECHNICAL TRANSLATION.** English-language translations of foreign scientific and technical material pertinent to NASA's mission.

Specialized services also include creating custom thesauri, building customized databases, organizing and publishing research results.

For more information about the NASA STI program, see the following:

- Access the NASA STI program home page at <http://www.sti.nasa.gov>
- E-mail your question via the Internet to help@sti.nasa.gov
- Fax your question to the NASA STI Help Desk at 443-757-5803
- Telephone the NASA STI Help Desk at 443-757-5802
- Write to:
NASA Center for AeroSpace Information (CASI)
7115 Standard Drive
Hanover, MD 21076-1320

NASA/TM—2010-216918



A Heat Transfer Investigation of Liquid and Two-Phase Methane

Jonathan Van Noord
Glenn Research Center, Cleveland, Ohio

Prepared for the
57th Joint Army-Navy-NASA-Air Force (JANNAF) Propulsion Meeting
sponsored by the JANNAF Interagency Propulsion Committee
Colorado Springs, Colorado, May 3–7, 2010

National Aeronautics and
Space Administration

Glenn Research Center
Cleveland, Ohio 44135

November 2010

Acknowledgments

The author would like to acknowledge the PCAD project for its support of this work. The author would also like to acknowledge Pratt & Whitney—Rocketdyne and Mr. Ben Stiegemeier of ASRC for their interactions and discussions about the data and testing.

Trade names and trademarks are used in this report for identification only. Their usage does not constitute an official endorsement, either expressed or implied, by the National Aeronautics and Space Administration.

Level of Review: This material has been technically reviewed by technical management.

Available from

NASA Center for Aerospace Information
7115 Standard Drive
Hanover, MD 21076-1320

National Technical Information Service
5301 Shawnee Road
Alexandria, VA 22312

Available electronically at <http://gltrs.grc.nasa.gov>

A Heat Transfer Investigation of Liquid and Two-Phase Methane

Jonathan Van Noord
National Aeronautics and Space Administration
Glenn Research Center
Cleveland, Ohio 44135

Abstract

A heat transfer investigation was conducted for liquid and two-phase methane. The tests were conducted at the NASA Glenn Research Center Heated Tube Facility (HTF) using resistively heated tube sections to simulate conditions encountered in regeneratively cooled rocket engines. This testing is part of NASA's Propulsion and Cryogenics Advanced Development (PCAD) project. Nontoxic propellants, such as liquid oxygen/liquid methane (LO₂/LCH₄), offer potential benefits in both performance and safety over equivalently sized hypergolic propulsion systems in spacecraft applications. Regeneratively cooled thrust chambers are one solution for high performance, robust LO₂/LCH₄ engines, but cooling data on methane is limited. Several test runs were conducted using three different diameter Inconel 600 tubes, with nominal inner diameters of 0.0225-, 0.054-, and 0.075-in. The mass flow rate was varied from 0.005 to 0.07 lbm/sec. As the current focus of the PCAD project is on pressure fed engines for LO₂/LCH₄, the average test section outlet pressures were targeted to be 200 psia or 500 psia. The heat flux was incrementally increased for each test condition while the test section wall temperatures were monitored. A maximum average heat flux of 6.2 Btu/in.² • sec was achieved and, at times, the temperatures of the test sections reached in excess of 1800 °R. The primary objective of the tests was to produce heat transfer correlations for methane in the liquid and two-phase regime. For two-phase flow testing, the critical heat flux values were determined where the fluid transitions from nucleate boiling to film boiling. A secondary goal of the testing was to measure system pressure drops in the two-phase regime.

Introduction

Developing new propulsion capabilities is imperative for the future of NASA's missions. These advances require performance improvements that would enable a lower system mass. Propellants that would allow for a lower system mass would result in a lower cost of vehicle development or allow for larger payloads. Propellants, such as liquid oxygen/liquid methane (LO₂/LCH₄), offer potential benefits in both performance and safety over equivalently sized hypergolic propulsion systems in spacecraft applications such as ascent stage engines or service module engines.

NASA's Propulsion and Cryogenic Advanced Development (PCAD) project is supporting experimental and analytical work into propulsion systems that use nontoxic propellants. The PCAD project is specifically developing LO₂/LCH₄ reaction control system thrusters, LO₂/LCH₄ ascent engines, and LO₂/LH₂ descent main engine development. One solution for high performance, robust LO₂/LCH₄ engines would be to use a regeneratively cooled thrust chamber, but cooling data on methane is very limited. This data is essential to properly design regenerative engines.

The primary objective for the investigation presented here was to produce heat transfer correlations for methane in the liquid and two-phase regime below critical pressure and appropriate for application to pressure-fed engines. For two-phase flow testing, critical heat flux values were determined where nucleate boiling transitions to film boiling. A secondary goal of the testing was to measure system pressure drops in the two-phase regime. To acquire this data, electrically heated tube tests were conducted for flow velocities from 8.1 to 157 ft/sec, outlet pressures ranging from 212 to 565 psia, inlet pressures ranging from 227 to 801 psia, and methane subcooling from 188 to 255 °R.

Test Facility, Hardware, and Procedure

Tests were conducted in the NASA Glenn Research Center Heated Tube Facility. This facility was developed for simulating the heat flux conditions of a regeneratively cooled liquid rocket engine combustion chamber and is described in Reference 1. The facility has been adapted to use liquid methane as the working fluid and the components used for this present investigation are summarized here.

Facility

A simplified schematic of the test setup is shown in Figure 1. The test section was mounted vertically inside a vacuum chamber with a maximum pressure of 0.01 psi (69 Pa). The vacuum environment prevented heat loss through convection and provided improved safety and containment if a test sample failed and resulted in a fuel leak. The test section was heated electrically by passing a current through the tube using a 1500 A, 100 V DC power supply. The methane was stored in a 16 gal insulated storage tank where the supply pressure was varied up to 1530 psia. For this test, the flow was controlled through the use of two cavitating venturis and a variation of supply pressures. It was observed that the venturis become partially obstructed during the testing, so while they controlled the flow, they proved to be inaccurate for calculating the flowrate. Therefore, the flow was measured using a turbine flow meter and recorded to an accuracy of ± 0.001 lbm/sec. The flow meter was calibrated for flows up to 1.5 gpm (~ 0.09 lbm/sec methane). The fluid temperature and pressure were measured at the inlet and exit of the test section to an accuracy of ± 4 °R and ± 0.4 percent, respectively. The heat input was determined by recording the voltage and current applied to the test section to an accuracy of ± 1 percent. The facility and research instrumentation were recorded on the facility's data system at a rate of one complete cycle per second.

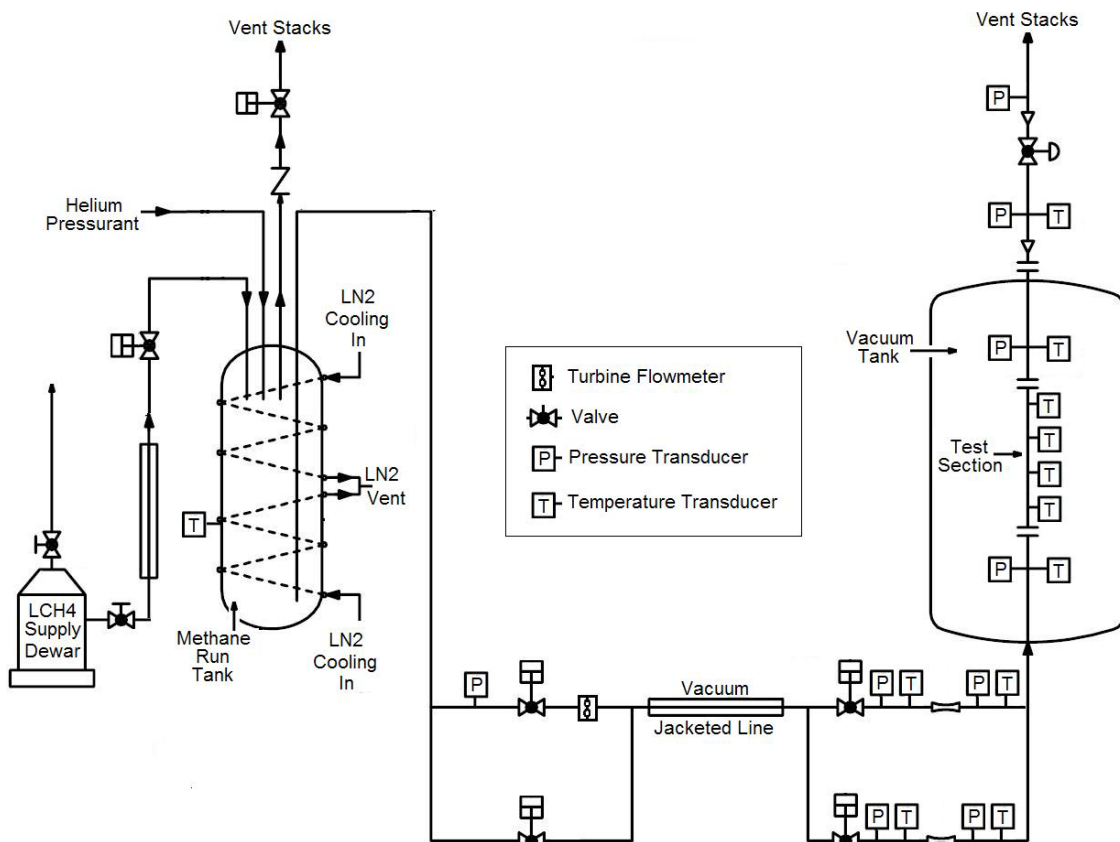


Figure 1.—Simplified test setup for Heated Tube Facility cryogen operation.

Test Hardware

There were four test sections fabricated out of Inconel 600 tubes with three different diameters. All of the test samples had wall thicknesses of 0.020 ± 0.002 in. The inner diameter of two of the samples was 0.083 in., one was 0.056 in., and one was 0.026 in. The varying diameters allowed for a variety of fluid velocities for a small number of mass flow rates. The test section with the smallest inner diameter of 0.026 in. had test section pressure drops up to 1000 psi and the data were not included in this paper. The total test section lengths were 14.5 in. and were connected to 0.25 in. tubing at the inlet. Each test section had 5 in. that was electrically heated. A length of 6.0 in. ($L/D > 100$) was provided before the start of the heated section to allow for flow development. Rectangular copper bus bars (1- by 3- by 0.25-in.) were brazed to the tube to provide electrical coupling to the power supplies.

The test sections were instrumented with type K thermocouples spot welded directly to surface of the tube. There were a total of 15 thermocouples on each test section with 11 on the heated section and two on the entrance and exit portions. The thermocouples were typically placed at 0.5 in. intervals in the heated section and 0.1 in. from each side of the bus bars. Figure 2 shows the typical arrangement of thermocouples. For the analysis presented in this paper, the wall thermocouples were primarily used to determine when the transition to film boiling occurred, also known as the critical heat flux.

Procedure

A typical test run started by cooling the 16 gal supply tank with liquid nitrogen flowing through tubing attached between the supply tank and insulation surrounding the tank. Once the supply tank was cooled to 260 °R, methane at 205 to 220 °R was transferred into the tank. The methane was then allowed to cool using LN₂ over a few hours to ≤ 190 °R. The boiling point of methane at atmospheric pressure is 201 °R. Once the methane was at the desired temperature, the supply tank was pressurized to 700 to 1500 psia with helium. At this point, the back pressure controller was set and the methane would flow until the sample reached a steady state temperature. The flow rate was adjusted by varying the supply tank pressure and allowing flow through one or both of the cavitating venturis. The test setup allows for parallel flow through two venturis for gross flowrate adjustments. The power supplies were then enabled and the power was incrementally increased with a pause to evaluate the response of the test section. Initially, there were many smaller incremental increases, but as the data was collected and confidence grew in the approximate value of the critical heat flux, the initial power steps were increased.

On most runs, the first objective was to determine the critical heat flux for a given condition. When the critical heat flux is reached, the temperature at one thermocouple (usually at the end of the heated section of the tube) shows a dramatic increase. Once the critical heat flux is reached, the power is immediately reduced to avoid damaging the sample. If it is not obvious that the critical heat flux is reached, as was typical with pressures > 450 psia, the power was increased until test section temperatures reached 1400 to 1800 °R. Once the critical heat flux was exceeded in this testing, the test section wall temperature typically increased on the order of 200 to 300 °F per second. Figure 3 shows the temperature of the furthest downstream thermocouple of the heated section, the average applied heat flux, and the outlet temperature that demonstrates this type of response. In some tests, the temperature achieved a steady state temperature below the material limits and power could continue to be added as shown in Figure 4. This slower response allowed for ample time to protect the test article from temperatures that could compromise its integrity, and there were no tube failures in this testing. Figure 5 is a typical plot showing the outer wall temperature at the end of the heated portion of the test section versus the applied heat flux. Initially during nucleate boiling, the temperature changes minimally for increasing heat flux, until film boiling is triggered and there is a rapid increase in wall temperature for a small amount of heat flux applied. Figure 6 shows what the test sample looked like when the critical heat flux is encountered.

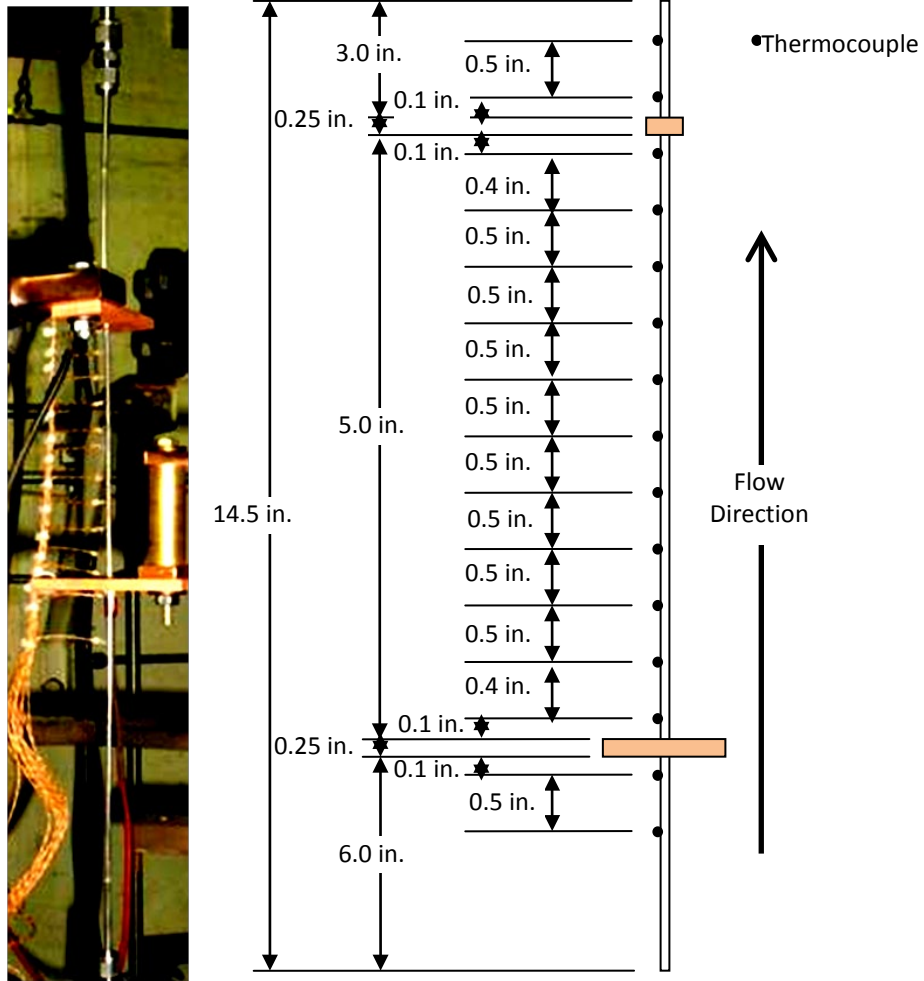


Figure 2.—Schematic and photograph of test section hardware and instrumentation. Figure not to scale.

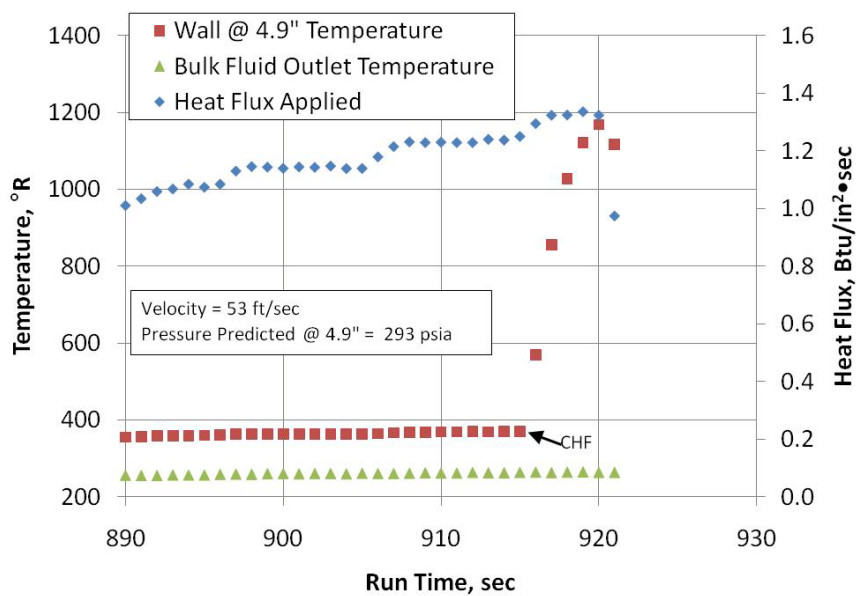


Figure 3.—Temperatures and heat flux profile demonstrating critical heat flux.

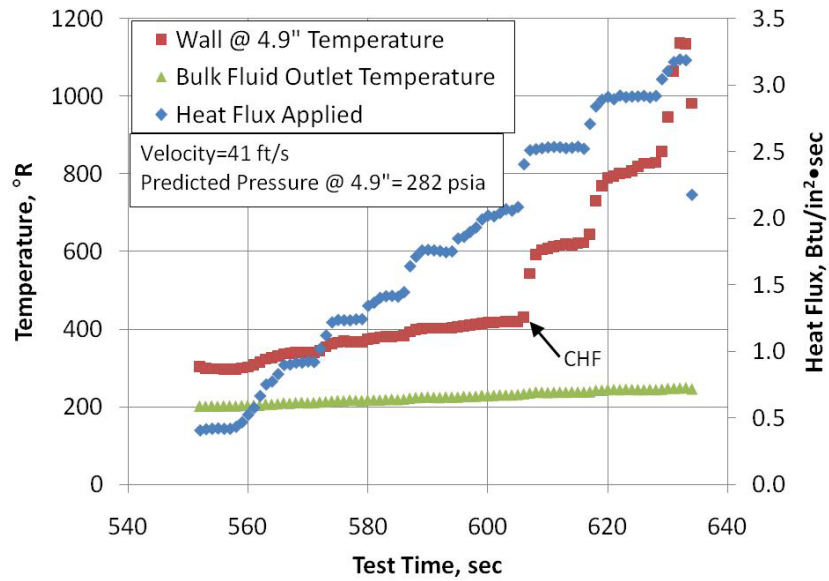


Figure 4.—Test case showing temperatures and heat flux prior to and after encountering the critical heat flux.

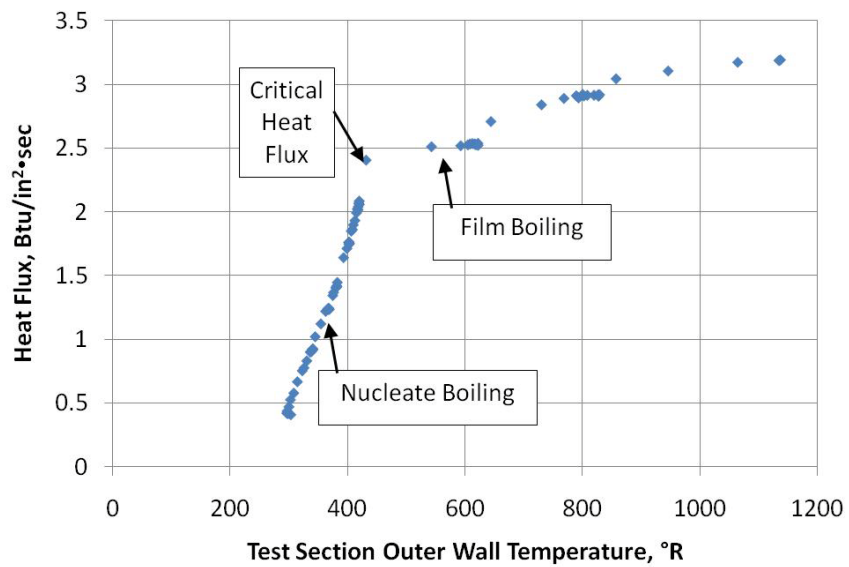


Figure 5.—Typical heat flux versus wall temperature showing the different modes of heat transfer with increasing heat flux.

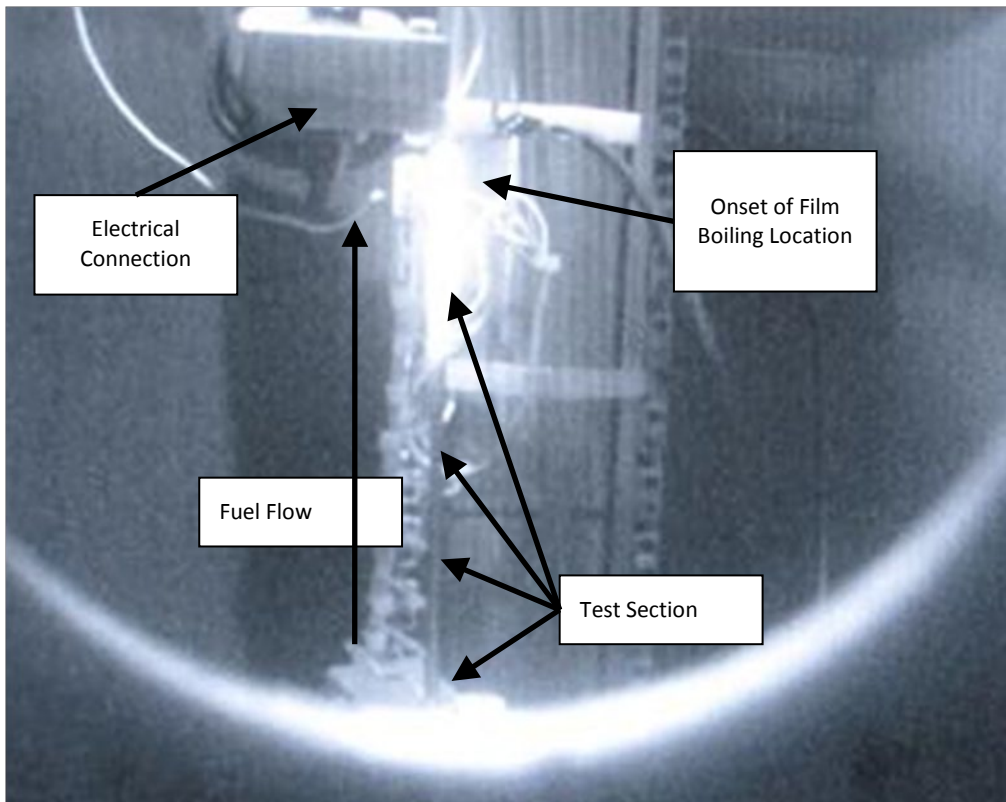


Figure 6.—An image of the test sample after the critical heat flux is encountered. Typically, the exit end of the test sample rapidly increased in temperature when the critical heat flux was encountered.

Results and Discussion

A summary of test conditions is given in Table 1. These test points represent either critical heat fluxes or the maximum heating for a given flow rate and pressure. Table 2 describes the test section diameters for the various test runs. The maximum heating occurred after transitioning through the critical heat flux or when the temperature on the test section wall exceeded 1400 °R when the critical heat flux was not obvious. During test runs 41 to 45, the flow meter failed, but the flow rates were estimated based on the pressure drops for that test sample. The pressure drop-flow rate relationship is shown in Figure 7.

TABLE 1.—SUMMARY OF TEST CONDITIONS AND RESULTS
 [Shaded cells are for test points with pressures at end of heated section < 300 psia.
 Test points correspond to critical heat flux or maximum heating achieved for a test run.]

Test run	Flow rate, lbm/s	Inlet		Outlet		ΔP , psi	Calculated at transition			Vel., ft/s	ΔT_{sub} , °F-ft/sec	Applied heat, Btu/in. ² sec	CHF point or outlet state†
		Temp., °R	Press., psia	Temp., °R	Press., psia		Press., psia	Bulk temp., °R	T_{sat} , °R				
1	0.047	216	270	259	236	34	249	259	291	47.2	1610	1.31	CHF
2	0.047	216	254	258	224	30	236	256	289	48.1	1690	1.23	CHF
3	0.044	214	257	268	231	26				44.4		1.49	L
4	0.016	228	234	274	225	8				16.4		0.95	2-phs
5	0.016	229	397	275	391	5				16.4		1.17	2-phs
6	0.013	244	522	316	518	4				12.7		1.16	2-phs
7	0.011	234	524	314	520	4				10.9		0.78	2-phs
8	0.051	211	272	259	273	-1	278	254	297	50.9	2280	1.39	CHF
9	0.050	211	271	263	273	-2				49.9		1.64	L
10	0.050	211	270	264	271	-1				49.9		1.65	L
11	0.049	208	568	253	571	-2	576	248	335	49.0	4320	1.23	CHF
12	0.046	208	565	306	570	-5				46.2		3.09	L
13	0.044	205	565	255	573	-7	575	252	335	43.4	3670	1.31	CHF
14	0.043	207	559	297	568	-7				43.4		2.56	L
15	0.044	207	276	254	281	-5	284	254	298	44.4	2030	1.36	CHF
16	0.043	206	272	259	278	-5				43.4		1.46	L
17	0.009	254	266	273	255	10				19.8		0.97	2-phs
18	0.068	200	779	259	290	497	455	258	322	148.6	9350	3.67	CHF
19	0.072	198	762	271	290	483				156.7		4.84	L
20	0.025	210	314	262	282	33	296	265	300	54.5	2030^	1.25	CHF
21	0.024	210	307	263	281	26				52.5		1.40	L/ 2-phs
22	0.024	212	312	263	280	32	293	268	299	52.5	1900^	1.24	CHF
23	0.023	212	309	265	280	30				40.4		1.34	L/2-phs
24	0.047	200	801	309	566	242				101.5		6.19	L/2-phs
25	0.037	207	697	262	577	121	619	273	339	79.1	6040^	2.25	CHF
26	0.036	200	699	299	585	118				77.0		3.96	L/2-phs
27	0.036	197	670	298	569	105				77.0		4.08	2-phs
28	0.038	196	709	318	542	172				81.1		5.11	L/2-phs
29	0.038	195	712	319	545	172				83.1		5.21	L/2-phs
30	0.021	200	601	315	543	59				44.3		2.62	L/2-phs
31	0.020	201	598	324	538	61				42.2		2.93	2-phs
32	0.025	201	318	264	240	79	264	268	294	54.5	1640^	1.54	CHF
33	0.042	191	466	255	243	227	314	262	302	91.3	4280^	2.73	CHF
34	0.041	192	461	255	241	222				89.3		2.79	L/2-phs
35	0.040	192	464	250	240	226				87.2		2.53	L/2-phs
36	0.040	192	461	256	238	227	307	265	301	87.2	3960^	2.73	CHF
37	0.040	191	453	256	240	215				87.2		2.83	L/2-phs
38	0.024	215	610	315	519	93				52.5		2.94	L/2-phs
39	0.042	199	478	256	222	259	300	262	300	91.3	4050^	2.46	CHF
40	0.040	199	474	257	217	259	293	268	299	87.2	3670^	2.61	CHF
41	0.030*	223	668	285	512	156	548	285	332	66.1*	3950^	2.52	CHF
42	0.025*	202	317	255	214	103	238	255	289	54.7*	1960^	1.60	CHF
43	0.025*	199	314	257	213	100	237	257	289	54.0*	1820^	1.63	CHF
44	0.028*	195	349	255	217	133	247	255	291	61.2*	2360^	1.90	CHF
45	0.022*	201	575	260	507	68	523	260	329	47.0*	3430^	1.47	CHF
46	0.046	197	276	248	217	60	235	261	289	45.3	1830^	1.89	CHF
47	0.035	198	255	250	215	40	227	266	287	34.1	1280^	1.49	CHF
48	0.035	198	545	248	510	35	518	329	329	34.1	2750^	1.40	CHF
49	0.054	194	591	298	515	78	538	324	331	52.7	1720^	5.02	CHF
50	0.052	195	575	300	501	76				50.9		5.20	2-phs
51	0.008	223	229	273	255	-26				8.1		0.89	2-phs
52	0.050	188	379	233	265	114	297	277	300	49.0	3260^	2.84	CHF
53	0.049	188	366	247	260	107				49.0		3.82	2-phs
54	0.041	191	330	234	262	68	282	282	297	40.6	2580^	2.41	CHF
56	0.041	191	345	249	279	66				41.6		3.19	2-phs

* Flows and velocities estimated based on the test section pressure drop

^When bulk temperature at transition exceeds outlet bulk, bulk temperature of outlet used to calculate ΔT_{sub} .

†CHF= Critical Heat Flux; L=Liquid; L/2-phs= Either Liquid or Two-Phase; 2-phs= Two-Phase

TABLE 2.—TEST SAMPLE DESCRIPTIONS

Test sample number	Inner diameter, in.	Outer diameter, in.	Test runs
1	0.083	0.127	1-19,51-56
2	0.056	0.0945	17-45
3	0.083	0.0127	46-50

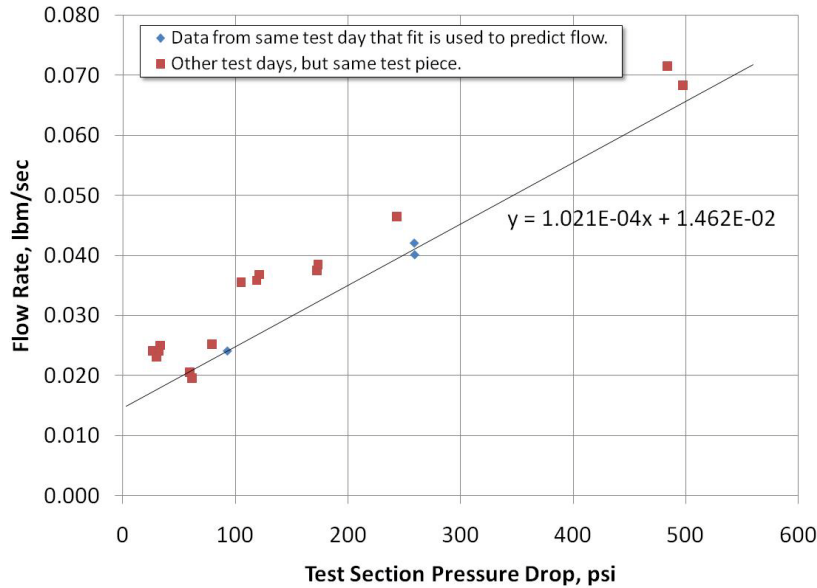


Figure 7.—Test section pressure drop compared to flow rate for Test Sample Number 2. Fit used to estimate flow for Runs 44 to 48 when flow meter failed.

Critical Heat Flux

The critical heat flux was determined for various velocities up to 149 ft/s. The change from nucleate to film boiling was quite pronounced for test section pressures less than 300 psia and Figure 3 to Figure 5 are representative of these behaviors. Figure 8 is a plot of the product of the flow velocity and subcooling $[Vx(T_{sat} - T_{bulk})]$ versus the critical heat fluxes for test sections less than 300 psia at the point of transition. These parameters have been successfully used to correlate other fuels as well as water (Refs. 2, 3, and 4). The saturation temperature used in the $V\Delta T_{sub}$ calculation is based on the pressure predicted at the transition point. The test section pressure is based on the measured inlet and outlet pressures and is determined by assuming a linear pressure decrease along the test section and with a pressure change as the fluid changes velocities from the larger ¼ in. fuel inlet line to the smaller diameter test section.

The fluid bulk temperature was determined using the average heat flux and flow rate to determine the amount the enthalpy increases from the measured inlet condition. The calculated pressure and enthalpy at a given location was then used to determine the fluid bulk temperature. The NIST standard reference database 23, version 7 was used to correlate temperature, pressure and enthalpy. Figure 9 shows the bulk temperature prediction based on this technique for one of the runs. In this case the bulk temperatures agree well. However, there were cases where the bulk temperatures predicted when heating began agreed well, but as the heating continued they substantially deviated. Figure 10 shows an example of this case. The model assumes that all of the heat flux added increases the fluid temperature until saturation temperature is reached and then two-phase flow occurs. This is also indicated by the prediction of quality that rises above zero corresponding to two-phase flow after 500 sec in Figure 10. The quality is calculated based on the outlet pressure and the calculated enthalpy.

However, it is speculated that the methane is vaporized into a gas hotter than the saturation temperature and does not condense back into the fluid by the time it passes the outlet pressure and

temperature instruments. This could result in a cooler fluid measurement than expected as shown in Figure 10. It should also be noted that for the case shown in Figure 10, it was with the largest diameter test section and the bulk temperature at the inlet is 25 to 30 °R cooler than the case shown in Figure 9. It is thought that these conditions have reduced the mixing effectiveness and resulted in this two-phase flow at fluid temperatures below saturation temperature. In the cases where the bulk temperature was predicted to be higher than the measured outlet temperature, the measured outlet temperature was used for the bulk temperature in the $V\Delta T_{\text{sub}}$ calculation. Figure 8 also includes the critical heat fluxes for runs where the flow was determined by the pressure drop. In those cases, the outlet bulk temperature was also used as the bulk temperature in the $V\Delta T_{\text{sub}}$ calculation.

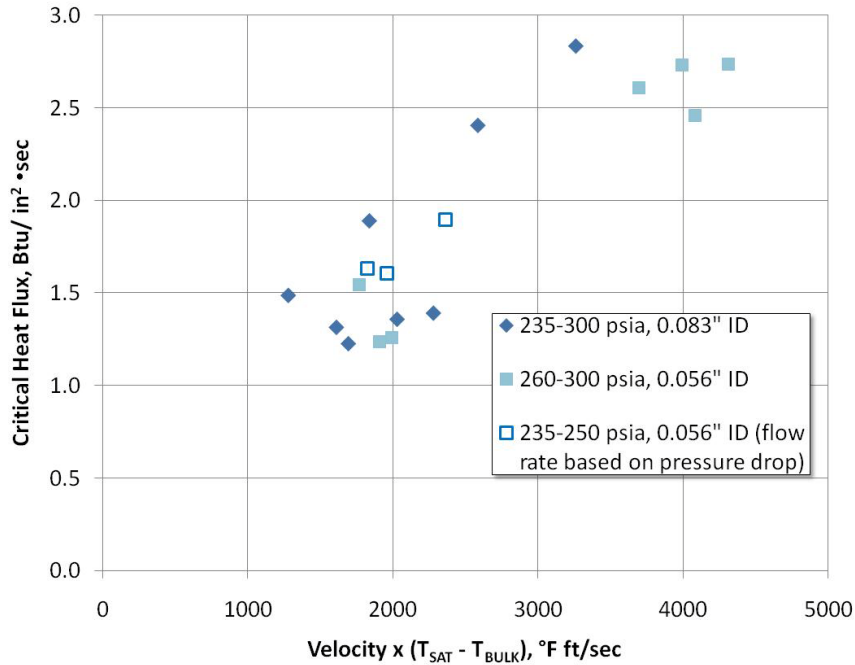


Figure 8.—Methane critical heat flux data for pressures from 235 to 300 psia. Flow rate for data represented by open squares determined by relationship shown in Figure 7.

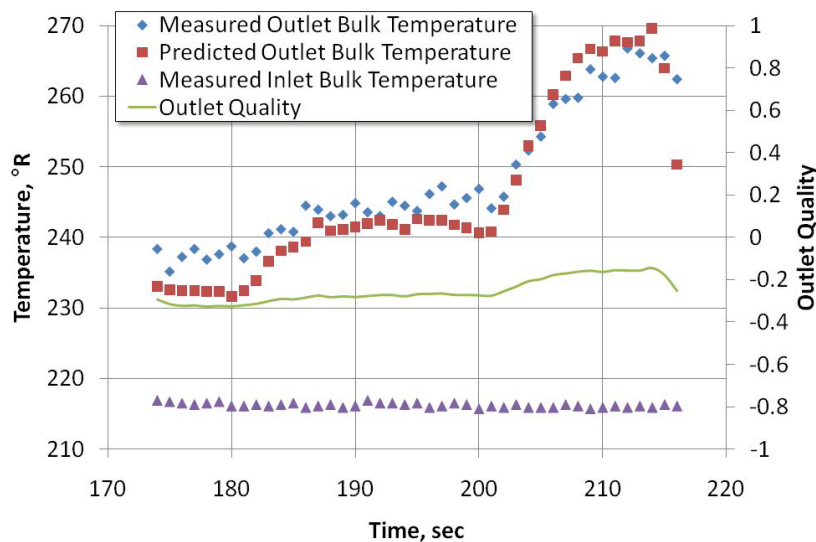


Figure 9.—Predicted bulk fluid temperature at the outlet along with fuel quality predicted based on enthalpy.

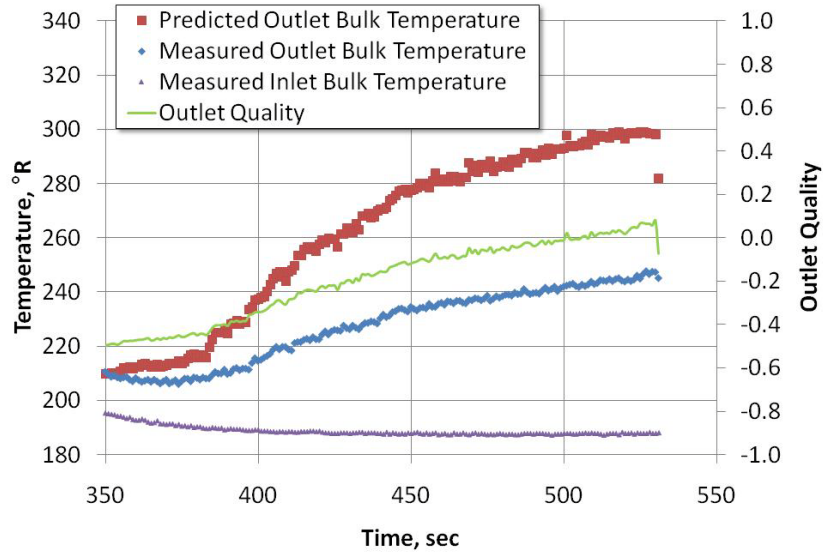


Figure 10.—Predicted bulk fluid temperature at the outlet along with fuel quality predicted based on enthalpy. A test run is shown with a larger difference between the predicted and measure bulk fluid temperature.

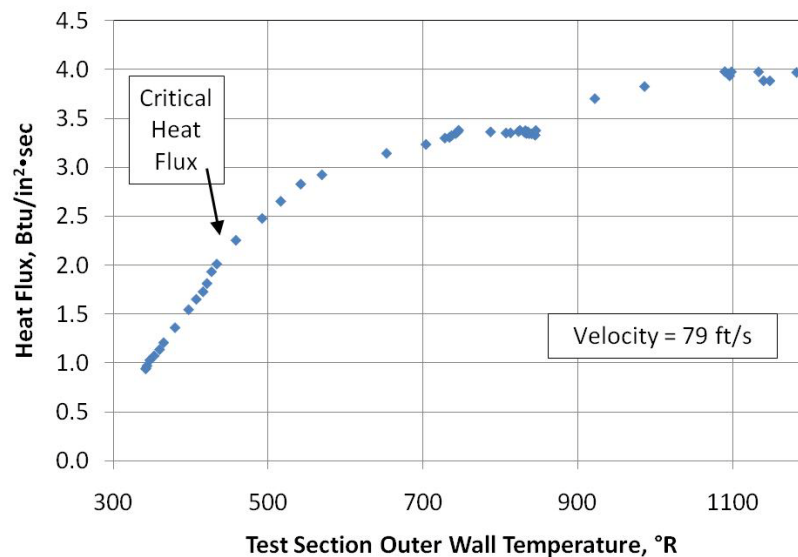


Figure 11.—Typical test section response for increasing heat flux with pressures higher than 450 psia. Critical heat flux is less obvious.

For test section pressures above 450 psia, the critical heat flux was less obvious. A plot of the test section outer wall temperature versus the heat flux is shown in Figure 11. At the higher pressures, the change in slope of the test section outer wall temperature versus the heat flux is gradual and does not have the same kind of “knee” as seen in Figure 5. The critical heat flux in this case is defined as the point when the slope changes. As seen in Figure 11, this is not a large change in slope, and almost double the heat flux was still able to be applied after the critical heat flux and before the test sample outer wall temperature reached 1100 °R. Figure 12 shows the critical heat flux correlation for the higher pressures.

As seen with other fluids, the higher pressure shifts the critical heat flux to higher $V\Delta T_{\text{sub}}$ (Ref. 2). The larger scatter in the data at higher pressure is largely due to the uncertainty of determining the transition from nucleate to film boiling as demonstrated in Figure 11. There were a comparable number of runs above 450 psia as there were from 235 to 300 psia, but fewer resulted in discernable critical heat flux points.

Pressure Drop

One way to evaluate the effect of two-phase flow on the pressure drop is to observe the change in pressure drop as heat flux is increased. Figure 13 shows representative pressure drop variations for two different flow rates, 0.041 and 0.051 lbm/s, as the heat flux is increased. Typically, for any test condition with a particular flowrate and pressure, the total pressure drop variation was on the order of 10 to 15 psi for all of the test runs. Figure 13 also shows the prediction of outlet quality as a function of heat flux for two test conditions. This is determined by the outlet pressure and the calculated outlet enthalpy. When the quality is above zero, it is predicted that there is two-phase flow with corresponding fraction equal to the amount of gas present. For example, 0.1 would mean that there is 10 percent gas phase present. A negative value corresponds to liquid only being present. It can be seen from Figure 13 that there is no significant change in pressure drop as two-phase flow develops. The slight decrease in the pressure drop for the 110 psi case shown when the quality is above 0.0 is not representative of other runs and is not a trend associated with two-phase flow. It is not clear at this point what contributed to the slight drop. Based on all the runs, two-phase flow does not appear to have a significant effect on the test section pressure drop.

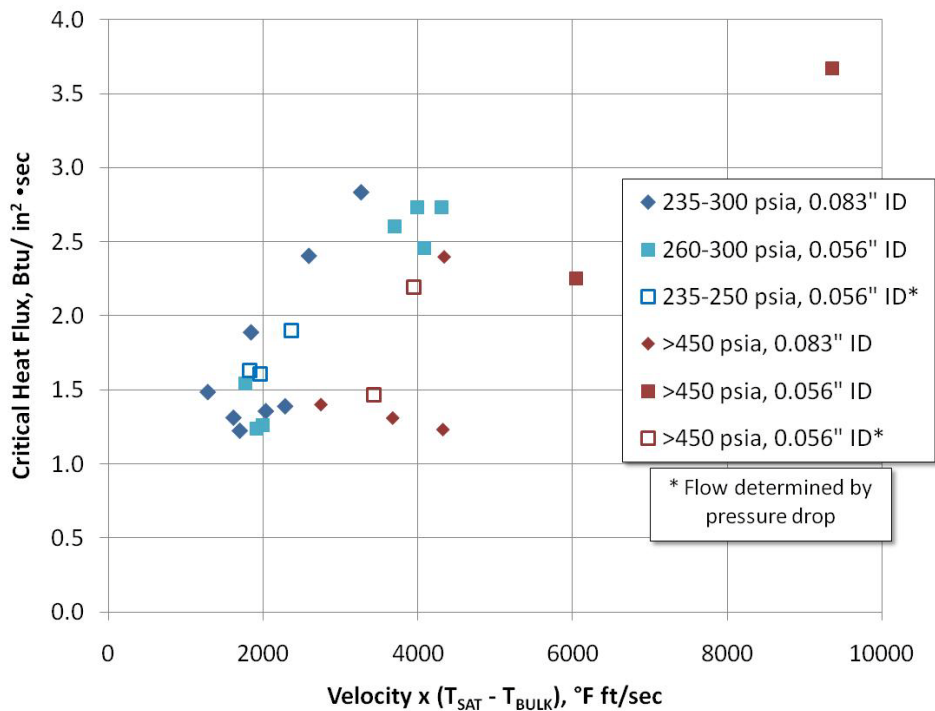


Figure 12.—Methane critical heat flux for various pressures. Flow rate for data represented by open squares determined by relationship shown in Figure 7.

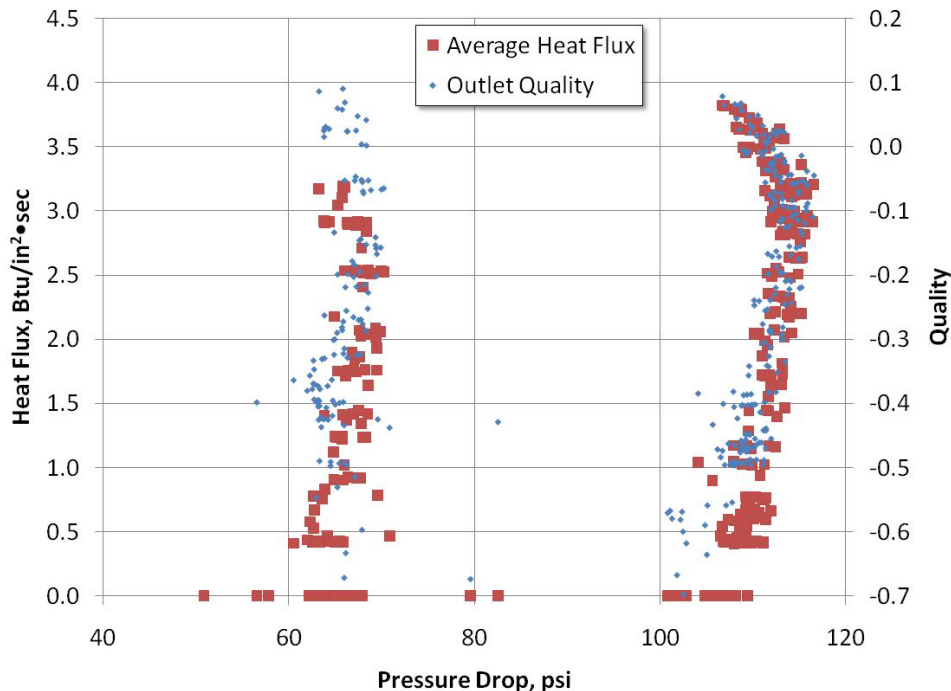


Figure 13.—Representative pressure drops as heat flux is increased represented by two different testing conditions. Test runs shown are for a 0.127 in. outer diameter sample with calculated transition pressures between 280 to 300 psia. The flowrate for the 65 psi pressure drop was 0.041 lbm/sec and the flowrate for the 110 psi pressure drop was 0.050 lbm/sec.

Summary and Conclusions

Testing with subcooled methane in electrically heated tubes was conducted. Fifty-six test points are presented comprised of flow velocities from 8.1 to 157 ft/sec, outlet pressures ranging from 212 to 565 psia, inlet pressures ranging from 227 to 801 psia, methane subcooling from 188 to 255 °R, and average heat fluxes up to 6.2 Btu/in.² • sec. Critical heat fluxes were determined and plotted as a function of $V\Delta T_{\text{sub}}$ from 1000 to 4000 °F ft/s for pressures from 235 to 300 psia. The change from nucleate to film boiling was quite pronounced for test section pressures less than 300 psia. Critical heat fluxes were also determined for pressures above 450 psia. The change from nucleate to film boiling was much more subtle for test section pressures above 450 psia. Instead of a sharp increase in wall temperature for a small amount of increased heat flux, as much as double the critical heat flux was applied before the test sample outer wall temperature reached 1100 °R. The total pressure drop variation for any test condition with a particular flowrate and pressure was on the order of 10 to 15 psi for the ranges of heat fluxes for any given test run. This indicates that two-phase flow did not appear to have a significant effect on the test section pressure drop, although predicted fluid quality did not exceed ~10 percent vapor.

References

1. Green, J.M., Pease, G.M., and Meyer, M.L., "A Heated Tube Facility for Rocket Coolant Channel Research," AIAA-95-2936, 1995.
2. Meyer, M.L., Linne, D.L., "Forced Convection Boiling and Critical Heat Flux of Ethanol in Electrically Heated Tube Tests," AIAA-98-1055, 1998.
3. Rousar, D.C., "Correlation of Burnout Heat Flux for Fluids at High velocity and High Subcooling Conditions," MS Thesis, University of California, Davis, 1966.
4. Greisen, D.A., and Rousar, D.C., "Critical Heat Flux Limits for High velocity, High Subcooling Water Flows," AIAA-97-2912, 1997.

REPORT DOCUMENTATION PAGE			Form Approved OMB No. 0704-0188		
<p>The public reporting burden for this collection of information is estimated to average 1 hour per response, including the time for reviewing instructions, searching existing data sources, gathering and maintaining the data needed, and completing and reviewing the collection of information. Send comments regarding this burden estimate or any other aspect of this collection of information, including suggestions for reducing this burden, to Department of Defense, Washington Headquarters Services, Directorate for Information Operations and Reports (0704-0188), 1215 Jefferson Davis Highway, Suite 1204, Arlington, VA 22202-4302. Respondents should be aware that notwithstanding any other provision of law, no person shall be subject to any penalty for failing to comply with a collection of information if it does not display a currently valid OMB control number.</p> <p>PLEASE DO NOT RETURN YOUR FORM TO THE ABOVE ADDRESS.</p>					
1. REPORT DATE (DD-MM-YYYY) 01-11-2010		2. REPORT TYPE Technical Memorandum		3. DATES COVERED (From - To)	
4. TITLE AND SUBTITLE A Heat Transfer Investigation of Liquid and Two-Phase Methane			5a. CONTRACT NUMBER		
			5b. GRANT NUMBER		
			5c. PROGRAM ELEMENT NUMBER		
6. AUTHOR(S) Van Noord, Jonathan			5d. PROJECT NUMBER		
			5e. TASK NUMBER		
			5f. WORK UNIT NUMBER WBS 253225.04.03.09.02.03		
7. PERFORMING ORGANIZATION NAME(S) AND ADDRESS(ES) National Aeronautics and Space Administration John H. Glenn Research Center at Lewis Field Cleveland, Ohio 44135-3191			8. PERFORMING ORGANIZATION REPORT NUMBER E-17494		
9. SPONSORING/MONITORING AGENCY NAME(S) AND ADDRESS(ES) National Aeronautics and Space Administration Washington, DC 20546-0001			10. SPONSORING/MONITOR'S ACRONYM(S) NASA		
			11. SPONSORING/MONITORING REPORT NUMBER NASA/TM-2010-216918		
12. DISTRIBUTION/AVAILABILITY STATEMENT Unclassified-Unlimited Subject Category: 20 Available electronically at http://gltrs.grc.nasa.gov This publication is available from the NASA Center for AeroSpace Information, 443-757-5802					
13. SUPPLEMENTARY NOTES					
14. ABSTRACT A heat transfer investigation was conducted for liquid and two-phase methane. The tests were conducted at the NASA Glenn Research Center Heated Tube Facility (HTF) using resistively heated tube sections to simulate conditions encountered in regeneratively cooled rocket engines. This testing is part of NASA's Propulsion and Cryogenics Advanced Development (PCAD) project. Nontoxic propellants, such as liquid oxygen/liquid methane (LO ₂ /LCH ₄), offer potential benefits in both performance and safety over equivalently sized hypergolic propulsion systems in spacecraft applications. Regeneratively cooled thrust chambers are one solution for high performance, robust LO ₂ /LCH ₄ engines, but cooling data on methane is limited. Several test runs were conducted using three different diameter Inconel 600 tubes, with nominal inner diameters of 0.0225-, 0.054-, and 0.075-in. The mass flow rate was varied from 0.005 to 0.07 lbm/sec. As the current focus of the PCAD project is on pressure fed engines for LO ₂ /LCH ₄ , the average test section outlet pressures were targeted to be 200 psia or 500 psia. The heat flux was incrementally increased for each test condition while the test section wall temperatures were monitored. A maximum average heat flux of 6.2 Btu/in.2 • sec was achieved and, at times, the temperatures of the test sections reached in excess of 1800 °R. The primary objective of the tests was to produce heat transfer correlations for methane in the liquid and two-phase regime. For two-phase flow testing, the critical heat flux values were determined where the fluid transitions from nucleate boiling to film boiling. A secondary goal of the testing was to measure system pressure drops in the two-phase regime.					
15. SUBJECT TERMS Cryogenic rocket propellants; Liquid propellant; Heat transfer; Methane					
16. SECURITY CLASSIFICATION OF:			17. LIMITATION OF ABSTRACT	18. NUMBER OF PAGES	19a. NAME OF RESPONSIBLE PERSON
a. REPORT	b. ABSTRACT	c. THIS PAGE			STI Help Desk (email:help@sti.nasa.gov)
U	U	U	UU	18	19b. TELEPHONE NUMBER (include area code) 443-757-5802

